Prediction of porosity in crystalline rocks using artificial neural networks: An example from the Chinese Continental Scientific Drilling Main Hole

AHMED AMARA KONATÉ[1], HEPING PAN[1*], NASIR KHAN[1] AND YAO YEVENYO ZIGGAH[2]

1 Institute of Geophysics and Geomatics, China University of Geosciences (Wuhan), Lu Mo Road 388, 430074 Wuhan, Hubei Province, China (konate77@yahoo.fr, panpinge@163.com)

2 Faculty of Information Engineering, China University of Geosciences (Wuhan), Lu Mo Road 388, 430074 Wuhan, Hubei Province, China

* Corresponding author

Received: October 28, 2013; Revised: February 17, 2014; Accepted: September 9, 2014

ABSTRACT

Porosity plays an important part of understanding permeability and fluid flow within the continental, crystalline rocks. Geophysical well logs are presently the most consistent means of providing continuous information for porosity estimation. However, it is difficult to interpret geophysical well logs data in crystalline rocks due to their complex geological features and the difficulty in understanding and using the complex and intensive information content in these data. Motived by the successful prediction abilities of artificial neural networks (ANN) to solve different problems in geophysics, this study explore the applicability of using ANNs to predict porosity in continental, crystalline rocks. This ANN technique is calibrated on Chinese Continental Scientific Drilling Main Hole (CCSD-MH) data, which provides core porosity data combined with four geophysical well logs (density, neutron porosity, sonic and resistivity). The data from CCSD-MH is utilized to train feed-forward backpropagation (FFBP) neural network and radial basis function (RBF) neural network to derive a relationship between geophysical well logs and porosity, and hence predict porosity accurately. The findings demonstrate that ANNs provide better performances with sets of three geophysical well logs (density, sonic and resistivity) than regression technique. Comparison of FFBP to RBF showed that RBF reveals better stability and more accurate performances than FFBP. Based on the success achieved in this study, this intelligence artificial technique can be a very advantageous tool in facilitating the task of geophysicists in the framework of research drillings in continental crust.

Keywords: geophysical well logs, geophysical exploration, computational geophysics, rock properties, neural networks, regression analysis, porosity prediction, crystalline rocks

1. INTRODUCTION

Many problems in geoscientific investigations can be solved by geophysical well logging (GWL). GWL involves the monitoring and evaluation of drilled rock from the earth's crust. It provides continuous records on the composition and structural features of the penetrated rock. In this context, rock properties such as, porosity can be estimated. GWL is widely used for reservoir evaluation in sedimentary environments (see *Serra, 2007*). Thus becoming the standard in hydrocarbon companies for the investigation of underground geology. Over time GWL has undergone significant improvement both in technique and data interpretation by oil companies for usage in sedimentary rocks. As a result, log responses in sedimentary environment are well known; even though, this is not the case for crystalline rocks (*Bartetzko et al., 2005*).

Crystalline rocks cover a wide spectrum of igneous, metamorphic and some sedimentary rocks in which the recrystallization process has been significant to their formation. These occur in a range of continental and oceanic settings, where a number of boreholes have been and continue to be drilled to provide greater insight into the composition, structure and processes of the earth's interior by means of geophysical surveys and geological mapping (*Harvey et al., 2005*). Knowledge in the use of well logging in crystalline rocks has been improved due to scientific research programs such as the International Continental Drilling Program (ICDP), Deep Sea Drilling Project (DSDP) and Ocean Drilling Program (ODP) (*Bartetzko et al. 2005*).

Immense investigations have been carried out by geoscientists based on crystalline rocks using well logging data (see *Anderson et al., 1990*; *Mooss, 1990*; *Pratsone et al., 1992*; *Pechnig et al., 1997, 2005*; *Luo and Pan, 2010*; *Pan et al., 2010*). The general understanding gathered from these research revealed that, the geophysical logs data from crystalline rocks are difficult to analyze because of their complicated geological characteristics and the difficulty in understanding and using the immense information content in these data. To overcome this problem, an efficient approach in studying crystalline rocks is the integration of information from both logs and core samples (*Pechnig et al., 1997*).

In this prevalent situation, artificial neural networks (ANN) offer various features that make them ideal systems for dealing with the complex and nonlinear geological problems of crystalline rocks from geophysical well data. ANNs are nonlinear systems, which makes them perfect for tackling nonlinearities in actual situations. The talent of ANNs to learn "input-output relationship" without prior information of the model structure makes them a very advantageous alternative to other modelling techniques. ANNs are appropriate approach when the dynamics of the problem is either unknown or too complicated. Furthermore ANNs have a high degree of fault tolerance against noise or errors in data. Therefore, ANNs are powerful and versatile systems with the capacity to deal with the complicated and nonlinear geophysical borehole records obtained so far from downhole crystalline crust such as the main hole of Chinese Continental Scientific Drilling (hereafter "CCSD-MH").

Innovative neural network tools have been successfully developed and utilized to solve logging problems (*Baldwin et al., 1990*; *Luthi and Bryant, 1997*; *Binaouda et al., 1999*; *Moritz et al., 2000*; *Bhatt and Helle, 2002*; *Zoveidavianpoor et al., 2013*) including research drilling in continental crust (*Maiti et al., 2007*; *Pan et al., 2010*; *Maiti and*

Tiwari, 2009, 2010). However, despite the existing literature, few papers are dedicated to neural networks in research drilling of continental crust especially in the case of Chinese Continental Scientific Drilling (CCSD). Therefore, the CCSD project well logs database creates an opportunity to apply and evaluate ANNs.

In terms of rock properties, geophysicists have undertaken several investigations on CCSD-MH. *Xu et al. (2000)* studied the velocity structures of the Sulu-Dabie orogeny and implications for seismic tomography. Using seismic refraction and reflection data *Kern et al. (2002)* measured the variation of P- and S-wave velocities from CCSD-MH. *Wang et al. (2004)* investigated on the P-wave velocities of eclogites by utilizing seismic properties. An analysis of the correlation between pretrophysical properties of ultra-high-pressure (UHP) metamorphic rocks from 100–3100 m of CCSD-MH was carried out by *Ou et al. (2005)*. In *Meng et al. (2007)* a preliminary investigation was done on paleomagnetism and rock magnetism of eclogite from the main hole. It was observed that all types of rocks have marked differences in their physical properties. At ambient temperature and hydrostatic confining pressures *Ji et al. (2007)* determined the P-wave velocities of UHP metamorphic rock samples collected from the CCSD-MH and from surface outcrops in the Sulu orogenic belt. *Luo and Pan (2011)* focused on Resistivity logs of the CCSD main drilled hole. The study showed that the resistivity of the UHP metamorphic rocks from the CCSD-MH is very high, because the porosity of the UHP metamorphic rocks is extremely low, and there are a few metal minerals dispersed within the rocks. In addition, *Sun et al. (2012)* carried out an investigation on P-wave velocity differences between surface-derived and core samples from the Sulu UHP metamorphic in order to compare the averages of P-wave velocities of four lithologies (felsic gneiss, eclogite, retrograde eclogite, and amphibolite) obtained from core materials sampled by the CCSD at depths to 5158 m, and from surface outcrops in the Dabie-Sulu UHP metamorphic.

Based on the above developments, the general understanding is that, 1) Most studies on rocks properties are carried out by the implication of seismic properties, and core samples from CCSD-MH and surface outcrops; 2) Data on *in situ* rock properties of CCSD-MH are still not fully exploited. The presented research suggests an approach for making a formulation between geophysical well logs and porosity. This approach takes into consideration all of the porosity indicators contained within geophysical well logs and integrates them into an association which perfectly predicts rock porosity.

Rock porosity is a petrophysical parameter utilized in many areas of geophysics. Porosity in crystalline rocks is often defined as the open space generated by fractures (*Tullborg and Larson, 2006*). It plays an important role in understanding permeability and fluid flow within the continental, crystalline rocks. There are no geophysical logs which can directly estimate porosity. Geophysical logs data provides only continuous information for porosity prediction. Therefore, the best source of porosity information comes from rock samples obtained from boreholes and measured in a laboratory (*Maiti and Tiwari, 2010*). However, the recuperation of cores is very expensive and is most often partial (*Chang et al., 2000*).

Several empirical relationships between porosity and geophysical well logs, such as density, sonic and neutron porosity have been formulated for sedimentary rocks. However, the conversion from these physical properties logs to equivalent porosity is not trivial (*Helle et al., 2001*; *Bhatt, 2002*). Hence, the applications of these empirical

relationships are limited. Following the same reasoning, *Pechnig et al. (1997)* indicated that due to the small porosities in crystalline crust, the performance of porosity predictions are poor. *Zimmermann et al. (1992)* developed statistical multiple regression models to predict porosity in crystalline rocks. Attempts have also been made by *Pechnig et al. (1997)* to predict porosity profiles using geophysical well log data from the German Continental Deep Drilling Program (KTB) drilled site. This was done using statistical methods such as linear regression, multiple regression and factor analysis. They mentioned that porosity predicted by statistical approaches overestimate the measured porosity at different ranges of depth. The main drawback of the statistical methodology are that the complex and nonlinearity of geophysical well logs can make statistical models complicated and awkward. This assertion has also been echoed by several authors such as *Maiti et al. (2007)* and *Maiti and Tiwari (2009, 2010)*.

In line with the above developments, the need for a consistent and high performance predicative approach is of particular importance in crystalline crust. The purpose of this investigation, consequently, is to develop an artificial intelligence based on ANNs for porosity prediction in crystalline crust by using geophysical logs data. This study demonstrates the efficiency of two types of ANN which include feed-forward backpropagation (FFBP) neural network and radial basis function neural network (RBF) for tackling accuracy estimation porosity problems in actual situations. Also of interest was the comparison of ANNs' results to those obtained by regression technique. The findings highlighted that the automated porosity prediction by ANNs with sets of three geophysical well logs (density, sonic and resistivity) can provide satisfying performance in the case of CCSD project.

2. ABOUT THE CHINESE CONTINENTAL SCIENTIFIC DRILLING

The Chinese Continental Scientific Drilling (CCSD) project was one of the largest and most expensive scientific research projects in geosciences ever undertaken in China. The Ministry of Land and Resources, the Ministry of Science and Technology, the National Natural Science Foundation of China, and the International Continental Scientific Drilling Program financed the project from the planning stage in 1999 through to end in 2007 (*Ji and Xu, 2009*). The CCSD-MH (34.40°N, 118.67°E) is located in the southern part of Donghai County (Jansu province), in the Sulu UHP metamorphic belt of Eastern China (Fig. 1).

The major scientific goal of CCSD project was to access the key composition, deep structure, and active processes of the Sulu UHP metamorphic belt that are not exposed, by means of drilling a hole into the continental crust. CCSD project has permitted testing of hypotheses and models derived from surface observations. Well logging was one of the most significant phases and key technologies in the CCSD project. The logging engineer employed more than 20 types of well logging tools and used advanced ECLIPS5700 image logging system to survey the entire section of the main hole, including resistivity laterolog, natural gamma ray, digital spectrometer (U, Th, K, SGR, CGR), litho-density, compensated neutron, multipole array acoustic log (V_p, V_s, V_{st}), simultaneous acoustic-resistivity image(Star-II), temperature, magnetic susceptibility, mud resistivity, Caliper, Inclinometer, etc. (*Niu et al., 2004*).The CCSD project which commenced in June 2001

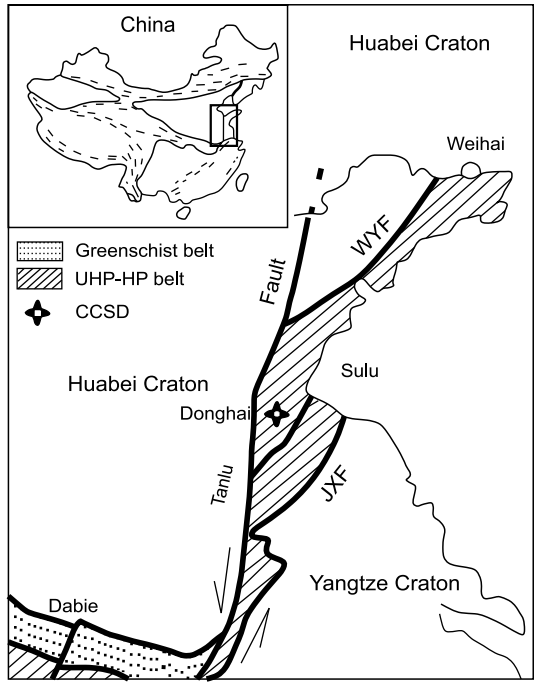

Fig. 1. Location of the Chinese Continental Scientific Drilling (CCSD) main hole (after *Yang, 2009*). WYF: Wuliang-Yantai Fault; JXF: Jiashan-Xionshui fault.

and reached its target depth of 5158 m in April 2005, has provided continuous records of physical and chemical data of the metamorphic rocks drilled.

3. GEOLOGICAL SETTING OF STUDY AREA

One of the most significant solid earth discoveries of the last three decades is the identification of a large ultra-high-pressure (UHP) metamorphic belt, more than 1000 km long, in the Sulu-Dabie region of central eastern China (*Xu et al., 2009*). This UHP metamorphic belt was first subducted into the mantle, and then quickly exhumed back up to the upper crust, producing the largest UHP metamorphic terrane in the world (see *Yang, 2009* and references therein). The Sulu-Dabie UHP metamorphic belt located at the east part of the Tanlu fault, resulted from the continental subduction and collision between the North China and the Yangtze cratons during the Triassic period (*Liu et al., 2010*, and references therein).The rocks on the surface outcrops in Dabie-Sulu are largely gneisses, comprising monzonitic gneiss, biotite gneiss and biotite plagioclase gneiss. These gneisses were constituted in the Proterozoic or older, and went through UHP metamorphism in the Triassic period; so the gneisses exhibited on the CCSD location frequently comprise coesite (*Liu et al., 2006*; *Yang, 2009*). The CCSD-MH is situated in the sigmoid shaped Maobei eclogite/ultramafic complex in the northern Sulu UHP upper tectonic slice (*Xu et*

al., 2009). Both coesite and diamond have been discovered in eclogite, and coesite has also been found in orthogneiss, paragneiss, quartzite and marble in the UHP metamorphic belt (*Xu et al., 2009*, and references therein).

Core sample from the CCSD-MH consists largely of granitic gneiss, paragneiss and eclogite or retrogressed eclogite, with less important amounts of amphibolite, ultramafic rock, and minor mica schist, mica-quartzschist, kyanite quartzite, granite and mylonite (*Xu et al., 2009*). The CCSD-MH is the deepest penetration (5158 m) drilled into extremely hard crystalline rocks such as eclogite, felsic gneiss, quartzite and garnet peridotite, nevertheless it is shallower than the Germany KTB (9101 m) and Russia Kola (12000 m) drilled holes respectively (*Ji and Xu, 2009*); and its crustal geology and lithology differ essentially from those sampled by KTB and Kola drilled holes (Ji and Xu, 2009). Information about CCSD project and its geological and geophysical implications can be found in several papers such as *Pan et al. (2002)*; *Niu et al. (2004)*; *Pan et al. (2005)*; *Ji and Xu (2009)*; *Xu et al. (2009)*; *Liu et al. (2010)*; *Luo et al. (2011)* and *Yang (2009)*.

4. DATA AND METHODOLOGY

The aim of this study is to convert geophysical logs data into porosity prediction by neural network modelling in crystalline crust. The available dataset for this work were the physical logs (see Table 1) and the porosity measurement from core samples of CCSD-MH. The logs evaluated in this research are bulk density (*DEN*), compensated neutron porosity (*CNL*), Sonic (*AC*), and spherically focused resistivity (*RSFL*). They were collected by Shengli logging company (*Pan et al., 2002*). The set of four geophysical logs selected for this study were considered to estimate porosity.

This paper focuses only on depths ranging from 101–2043 m where available core porosity measurement exist. We have combined core porosity data with the corresponding values of four geophysical well logs data in CCSD-MH where they were effective at the same depth (see example in Table 2). A total of 325 data points, collected from the depth interval 101–2043 m were used in this study to obtain an approximation of the relation between porosity and geophysical well logs.

To obtain the results presented in this paper, the steps of the methodology are described in the following sections.

Table 1. List of geophysical well logs used in this study.

Parameter	Method	Symbol	Unit
Compressional wave travel time	Sonic	*AC*	μs/m
Compensated neutron porosity	Neutron absorption	*CNL*	p.u
Bulk density	Gamma ray scattering	*DEN*	g/cm^3
Spherically Focused Resistivity	Electrical resistivity	*RSFL*	Ωm

Table 2. Example of core porosity data associated with values of four well logs at corresponding depths. See Table 1 for the parameters.

Depth [m]	*RSFL* [Ωm]	*CNL* [p.u]	*AC* [μs/m]	*DEN* [g/cm^3]	Porosity [%]
163.35	1716.56	3.27	50.60	3.29	1.00
167.20	3244.64	4.66	45.41	3.28	1.46
172.35	2157.60	4.17	47.86	3.33	1.44
178.97	2680.57	4.12	48.10	2.89	1.58
184.65	3406.28	2.39	50.06	2.87	1.55
189.53	1604.16	3.72	44.94	3.39	1.66
193.90	3466.52	3.18	50.79	3.34	1.32
199.70	3225.35	2.93	43.55	3.34	2.11
211.40	2371.55	3.82	47.15	2.98	1.38
218.90	2353.18	2.02	48.84	2.85	1.55
222.60	2614.76	3.08	47.91	3.31	1.58
229.90	3464.26	5.18	48.89	3.18	1.30
236.86	1499.99	5.01	52.88	3.52	1.68
238.50	2800.33	3.45	49.36	3.32	1.46
248.26	2035.99	3.21	52.08	3.17	1.43
250.55	1720.68	1.55	52.76	2.82	1.35
255.90	2361.57	2.54	49.53	3.03	1.07
261.26	2463.44	2.61	52.03	3.17	1.52

4.1. Data processing and identifying inputs parameters

One of the factors affecting the performance of ANNs is related to the quality of dataset used in model-building (*Dreiseitl and Ohno-Machado, 2002*). Therefore, the first step considered was the well data processing. An important observation made by *Luo and Pan (2010, Fig. 4)* was that the cavings and breakouts of CCSD-MH caused many anomalies on well log data. Therefore, in this study all geophysical well log data which exhibited strange, and possibly incorrect data were ignored, so that the geophysical log data can be used successfully to predict porosity using a computational neural networks. In addition, correction of the matching between core depth and logging depth was done, so that the geophysical well logs and experimental data may be matched and integrated effectively.

In the second step, the inputs (geophysical logs) should be identified for training ANNs. In this regard, the relationship between inputs and output (measured porosity) is required for identifying the potential input geophysical logs. The input data should represent the condition for which training of the neural network is done. All input neurons should represent some independent variable having an impact over the output of the neural network. Moreover the neural network has to be constructed in such a manner that the application of set of inputs produces the desired set of outputs. In this light, Pearson correlation coefficients were calculated in order to extract statistical significant relationships between measured porosity and geophysical logs.

Pearson correlation coefficient $R(x,y)$ is given as

$$R(x,y)=\frac{\sum(x_i-\bar{x})(y_i-\bar{y})}{\sqrt{\sum(x_i-\bar{x})^2\sum(y_i-\bar{y})^2}}, \tag{1}$$

where x_i and y_i are the i-th values and $\bar{x}$ and $\bar{y}$ are the mean values of the x and y variable, respectively.

4.2. Normalization

The third step was to adequately normalize the selected inputs so that the ANNs will provide good results and the calculation time will be significantly reduced. In this study, the selected inputs variables were normalized in [0, 1] using scaled value

$$x_k^*=\frac{x_i-\min(x)}{\max(x)-\min(x)}. \tag{2}$$

4.3. ANNs architecture

The ANNs models that are popular and appropriate in function approximation are FFBP and RBF respectively. They are multilayer, feed-forward and fully connected neural network. Their architecture details are described in Section 5. As mentioned by *Van der Baan and Jutten (2000)*, there is no theory expanding the present state of knowledge to determine the optimal architecture of a network. Therefore, in this study, it was fixed in an experimental manner, but the knowledge of the problem, the intuition of the user and the ability to experiment with several architectures can often make good assumptions.

4.4. Network training

We aimed to find an approximation of the relationship between porosity (Φ) and selected well logs, i.e. $\Phi = f(\text{selected well logs})$. Based on collected data, ANNs were trained to generate the preferred input-output relationship. A FFBP was trained using Levenberg-Marquardt algorithm; RBF was trained both by unsupervised (*k*-mean clustering and *P* nearest-neighbor) and supervised (gradient descent rule) methods. These training methods details are described in Section 5.

Besides, dataset was divided in two independent part. The first 228 data points were used for training the networks. While the remaining data points were used for testing.

The two networks (FFBP and RBF) were allowed to learn until no additional effective improvement occurred. After training the networks, testing data was used to evaluate the prediction ability of the ANNs. The two trained networks were then used to interpret the porosity profile of CCSD-MH. Only the results released by the best performing model was included in this study.

4.5. Performance indicators

The mean squared error (*MSE*) and coefficient of determination (R^2) between the observed and predicted porosity belong to training and testing data are the utmost

common indicators to offer a quantitative description of the goodness of the model predicted. They are given as

$$MSE = \frac{1}{N}\sum_{i=1}^{N}\left(\Phi_{oi} - \Phi_{pi}\right)^2, \tag{3}$$

$$R^2 = \left(\frac{\sum_{i=1}^{N}\left(\Phi_{oi} - \bar{\Phi}_o\right)\left(\Phi_{pi} - \bar{\Phi}_p\right)}{\sqrt{\sum_{i=1}^{N}\left(\Phi_{oi} - \bar{\Phi}_o\right)^2 \times \sum_{i=1}^{N}\left(\Phi_{pi} - \bar{\Phi}_p\right)^2}} \right), \tag{4}$$

where Φ_{oi} and Φ_{pi} are the *i*-th measured and predicted porosity values, respectively, $\bar{\Phi}_o$ and $\bar{\Phi}_p$ the respective mean values. *MSE* measures the average of the squares of the errors, i.e. the residual errors, which helps scientists to understand and interpret the difference between the observed value and estimated values. We should keep in mind that this indicator measures how near a fit line is to data points. The smaller the *MSE*, the nearer the fit is to the data points. R^2 is a statistical index that expresses the quality of fit estimates of the regression equation and also the intensity of the linear relationship. It helps to have a general idea of the model fit. Its value varies between 0 and 1, and if the R^2 value is close to 1 it is sufficient to say that the fit is good.

5. ARTIFICIAL NEURAL NETWORKS APPROACH

An ANN is a system of programs and information structures that mimics the operation of the human brain; it involves a large number of processors (neurons) operating in parallel to solve a specific problem (*Baddari et al., 2009*). Each unit (neuron) takes many input signals, then, based on an interior weighting organization, produces a single output signal that is typically sent as an input to another neuron. The units are interconnected and organized into different layers.

ANNs are computational modeling tools that have been widely utilized in different areas of geophysics to model, analyze and solve complex problems (see *van der Baan and Jutten, 2000*; *Poulton, 2002*). ANNs applications in logging data analysis can be classified according to two major features; 1) by the type of problem they can resolve (either classification or prediction) and 2) by the type of training used (supervised or unsupervised). The approach taken in this paper is supervised training for prediction. Supervised learning i.e. guided learning by "teacher"; needs training data which consists of input vectors and a target vector connected with each input vector. The advantage of supervised training is that the output can be interpreted based on the training values.

This study has developed and optimized two neural network approaches for porosity predictive model. They are feed-forward backpropagation (FFBP) neural network and radial basis function neural network (RBF). ANNs such as FFBP and RBF have been

proved to be universal function approximators (*Park and Sandberg, 1993*; *Benoudjit and Verleysen, 2003*).

5.1. Feed-forward backpropagation (FFBP) neural network

FFBP is the most common neural network, with the utmost application in geophysics among all other types of neural networks. This is due to their simple structure design, robust capability, and availability of a large number of training algorithms. This method also goes by several other names, such as backpropagation neural network (BPNN) and multi-layer perceptron (MLN). A FFBP consists of a layer of input units (neurons), one or more layers of hidden units, and one layer of output units. Characteristically, the layers are entirely interconnected. Fig. 2 shows a FFBP with only one hidden layer.

Choice of the number of hidden layers, hidden neuron and type of transfer function plays an important role in model constructions (*White, 1992*). Based on literature on FFBP, in majority problems, only one hidden layer is sufficient. *Hornik et al. (1989)* proved that FFBP with one hidden layer is enough to approximate any continuous function. Therefore, one hidden layer was employed in the current research. Besides, transfer functions for the hidden nodes are needed to introduce nonlinearity into the network. In this study, the hyperbolic tangent was selected as activation function of the hidden neurons while a linear activation function was used in the output neurons. The general form of the hyperbolic tangent is given as

$$f(S) = \frac{e^{S} - e^{-S}}{e^{S} + e^{-S}}, \tag{5}$$

where S is the sum of the weighted inputs. Further, the optimal number in hidden layer was selected by experimental trial based on the smallest mean squared error (*MSE*.)

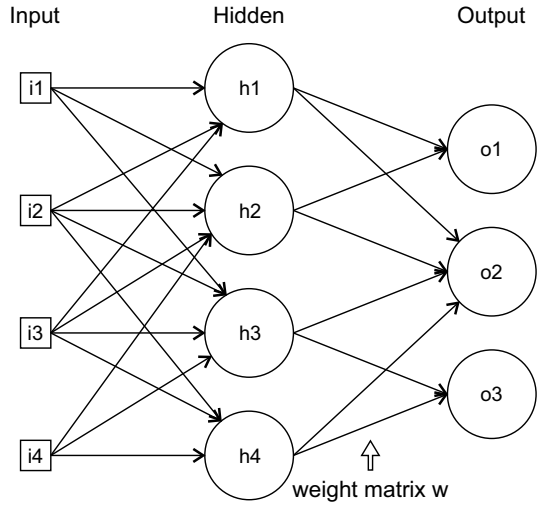

Fig. 2. Scheme of a feed-forward backpropagation neural network with only one hidden layer. i - input neurons, h - hidden neurons, o - output neurons.

The objective of training the FFBP is to find optimal connection weights (w^*) in such a manner that the calculated outputs value for each example matches the desired outputs value. This is typically a nonlinear optimization problem, where w^* is given as

$$w^* = \arg\min E(\mathbf{w}), \tag{6}$$

where $\mathbf{w}$ is weight matrix and $E(\mathbf{w})$ is an objective function on $\mathbf{w}$, which is to be minimized. The $E(\mathbf{w})$ is evaluated at any point of $\mathbf{w}$ as follows:

$$E(\mathbf{w}) = \sum_p E_p(\mathbf{w}), \tag{7}$$

where p is the number of examples in the training set and $E_p(\mathbf{w})$ is the output error for each example p and is defined as

$$E_p(\mathbf{w}) = \frac{1}{2}\sum_j \left(d_{pj} - y_{pj}(\mathbf{w})\right)^2, \tag{8}$$

where $y_{pj}(\mathbf{w})$ and d_{pj} are the calculated and desired network outputs of the j-th output neuron for p-th example, respectively. Substituting Eq. (8) into Eq. (7) we get

$$E(\boldsymbol{w}) = \frac{1}{2}\sum_p \sum_j \left(d_{pj} - y_{pj}(\mathbf{w})\right)^2. \tag{9}$$

For each learning (training) process, the network calculated output value is compared to the desired output value. If there is a difference between the calculated and desired output network, the synaptic weights which contribute to generate a significant error will be changed more significantly than the weight that led to a marginal error. The adaptation of the weights begins at the output neurons and then continues towards the input data. There are many algorithms available to perform this weight selection and adjustment (see *Bishop, 1995*).

In our study, Levenberg-Marquardt algorithm (LMA, *Levenberg, 1944*) was chosen to train the neural network, because LMA is considered as one of the most efficient training algorithms. The study of *Hagan and Menhaj (1994)* proved that LMA is faster and has more stable convergence. LMA is a Hessian based algorithm for nonlinear least squares method. Hessian based algorithms are utilized to allow ANNs to learn more suitable features of a complex mapping (*Isa et al., 2010*). The LMA for updating weights, $\mathbf{w}$, can be presented as (*Reynaldi et al., 2012*)

$$\mathbf{w}_{k+1} = \mathbf{w}_k - \left(\mathbf{J}_k^{\mathrm{T}}\mathbf{J}_k + \mu\mathbf{I}\right)^{-1}\mathbf{J}_k^{\mathrm{T}}\boldsymbol{e}_k, \tag{10}$$

where $\mathbf{w}_k$ is the current weight, $\mathbf{w}_{k+1}$ is the next weight, $\mathbf{J}$ is the Jacobian matrix, which contains first derivatives of the network errors with respect to the weights; $\boldsymbol{e}$ is a vector of network errors; $\mathbf{I}$ is identity matrix and parameter μ is a scaler whose value is always positive. This parameter depends on evaluation of the sum of squared errors. The LMA starts the minimization process with a large value of μ, thus approximating a gradient descent algorithm. As the algorithm approaches a solution, μ decreases. When the value

of μ is very small (nearly zero), LMA is equal to the Gauss-Newton algorithm, where a search direction is obtained at each iteration. The search direction is the solution to the linear least squares problem.

5.2. Radial basis function (RBF) neural network

RBF is a type of ANN which has a feed-forward structure. It consists of an input layer, a single hidden layer and an output layer. Each layer is completely linked with the following one (Fig. 3). Here, the connections between the input and the hidden layers are unweighted. The inputs thus reach the hidden layer nodes (units) unchanged. Only the connections between the hidden layer and the output layer are weighted, leading to a much faster training rate. The main differences between FFBP and RBF networks are that in the RBF the connections between the input and hidden layer are unweighted and the activation functions on the hidden layer neuron are radially symmetric.

The response characteristics ϕ_j of the hidden units *j* are given by (*Celikoglu, 2006*)

$$\phi_j = \psi_j \left(\frac{\left\| \boldsymbol{x} - \boldsymbol{z}_j \right\|}{\sigma_j^2} \right). \tag{11}$$

Each hidden unit output is obtained by computing the closeness of the input to an *n*-dimensional parameter vector $\boldsymbol{z}_j$ associated with the center of the *j*-th hidden unit, where $\boldsymbol{x} \in R^n$ is the input vector and σ_j the width coefficient for hidden unit *j*, which represents a measure of the data spread. $\left\| \boldsymbol{x} - \boldsymbol{z}_j \right\|$ is a norm of $\boldsymbol{x} \to \boldsymbol{z}_j$, which represents the distance

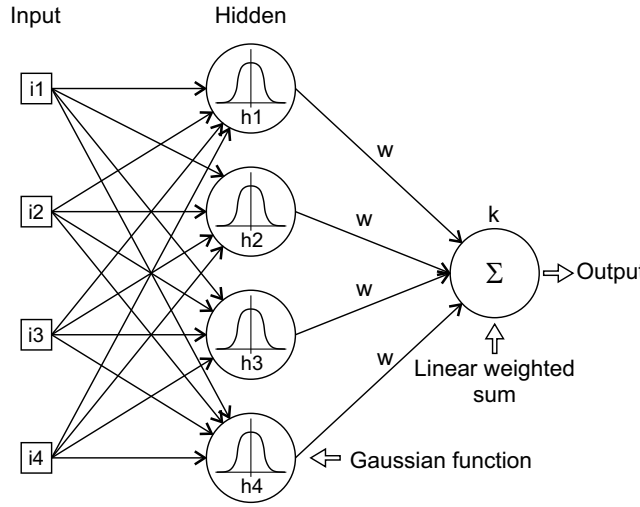

Fig. 3. Scheme of a radial basis function neural network with only one hidden layer. i - input neurons, h - hidden neurons, k - output neuron, w - synaptic weights.

between the input vector $\boldsymbol{x}$ and z_j. In this study the Euclidean norm is used. ψ_j is a radially symmetric function, which achieves the unique maximum at the point of z_j. With the increase of $\|\boldsymbol{x}-\boldsymbol{z}_j\|$, ψ_j rapidly attenuates to zero.

In an RBF, the output neurons only contain the identity as transfer function and one weighted sum as propagation function. Then the network output for $\boldsymbol{x} \in R^n$ and $\sigma \in R^M$ can be expressed formally as (*Celikoglu, 2006*):

$$\hat{y}(\boldsymbol{x}, \boldsymbol{z}, \sigma, \boldsymbol{w}) = \sum_{k=1}^{M} \boldsymbol{w}_k \phi(\boldsymbol{x}, \boldsymbol{z}_j, \sigma_j), \tag{12}$$

where $\phi(\boldsymbol{x}, \boldsymbol{z}_j, \sigma_j)$ is the *j*-th function with center $\boldsymbol{z}_j \in R^n$, width σ_j, and $\boldsymbol{w} \in R^M$ is the vector of linear output weights.

Although the choice of the basis function is not crucial to the performance of the network (*Chen et al., 1991*), the most common is the Gaussian function. In this study the Gaussian function was employed as function basis for the hidden units.

The training of RBF was based on using a hybrid procedure proposed by *Moody and Darken (1989)* consisting of both unsupervised and supervised learning methods. Training of the hidden layer involves the calculation of the radial basis functions by identifying suitable $\boldsymbol{z}_j$ and σ_j for each neuron. These parameters are dependent only on the inputs and are independent of the outputs, making this section of the learning process an unsupervised one. In this light, the radial basis neuron centers $\boldsymbol{z}_j$ were determined using *k*-means clustering. This algorithm find sets a *k* neuron centers which represent a local minimum of the total squared Euclidean distances between the training vectors and the neuron centers.

The next stage of the unsupervised training process concerned the neuron widths σ_j, which are determined using a *P* nearest-neighbor heuristics. This technique varies the widths to achieve a certain amount of response overlap between each neuron and its *P* nearest neighbors. In supervised learning, the output layer was trained by gradient descent learning rule in which the weights are updated in proportion to the difference between the network output and the target output.

6. RESULTS AND DISCUSSION

In order to investigate input parameters which are suitable for the ANNs models, an analysis was conducted using Pearson correlation. Table 3 highlights the relationship between geophysical logs and measured porosity. As shown in Table 3, Pearson correlation analysis assumes that the relationships existing between *RSFL*, *DEN*, *AC* logs and measured porosity respectively are statistically significant. However, it underestimates the strength of these relationships. This fact is reflected by existence of nonlinear relationship between these variables. In line with this, we supposed that there must exist a relationship between well logs (*RSFL*, *DEN* and *AC*) and measured porosity. Therefore in this study *RSFL*, *DEN*, *AC* were selected as inputs parameters of the ANNs

Table 3. Pearson correlation coefficient *r* of core measured porosity versus geophysical well logs data using all data.

	r	*r* Probability (*p*)	Level of Significance
Measured porosity vs RSFL	0.385*	0.000	0.01
Measured porosity vs AC	0.200*	0.000	0.01
Measured porosity vs DEN	0.220*	0.000	0.01
Measured porosity vs CNL	0.033	0.554	0.01

* Correlation is statistically significant at the 0.01 level (2 tailed).

The next step was to find an approximation of the relationship between porosity (Φ) and *RSFL*, *DEN*, *AC*: $\Phi = f\left(RSFL, DEN, AC\right)$ by using ANNs which include FFBP and RBF. We supposed that, the shape of the function *f* appears to be nonlinear. Accordingly, ANNs are highly nonlinear, hence having mapping abilities to approximate *f* without a priori knowledge.

The inputs parameters (*RSFL*, *DEN* and *AC*) and output (measured porosity) have been scaled to the interval [0, 1]. The FFBP used here consists of three inputs, one hidden layer using the hyperbolic tangent as activation function and one output layer using linear activation function. While RBF consists of three inputs, one hidden layer using Gaussian function as activation function and one output layer using linear activation function.

In order to determine the optimal network structure to predict porosity data in the examined CCSD-MH, resulting from the procedure described in the previous section, several networks were trained and tested. After some trials, it was found that the optimal network for FFBP was one hidden layer of 10 units. While the optimal RBF was one hidden layer of 15 radial basis units.

Figure 4 clearly depict the closeness of fit of these two schemes learning, respectively, to the observed porosity from training data. The findings in Table 4 additionally confirm the quality of the learning performances, since both FFBP and RBF scheme show high R^2 values. Considering again the findings in Table 4, RBF scheme exhibits higher R^2 value and lower *MSE* value than FFBP scheme, indicating that satisfactory training was achieved by the RBF scheme. Therefore, in this study, RBF scheme appears to perform slightly better than FFBP scheme, which obviously indicates that the RBF has learning power.

After end of the training phase, the testing phase took place. The plot of the FFBP and RBF schemes from testing data are depicted in Fig. 5. The statistical assessment criteria achieved by the network using testing data (*MSE* and R^2) are presented in Table 5. As can be deduced from Fig. 5, both FFBP and RBF scheme closely predict observed porosity and appear to follow observed porosity as well indicating that these networks were well-developed. The result in Table 5 exhibits the better prediction ability of the RBF model than FFBP model, as, RBF shows lower *MSE* value and higher R^2 value; while FFBP highlights higher *MSE* value and lower R^2 value. A high R^2 value indicates that a majority of the variability in the porosity could be explained by the three geophysical well logs (*RSFL*, *DEN* and *AC*). This means that RBF demonstrates close relationships between porosity and the three geophysical logs.

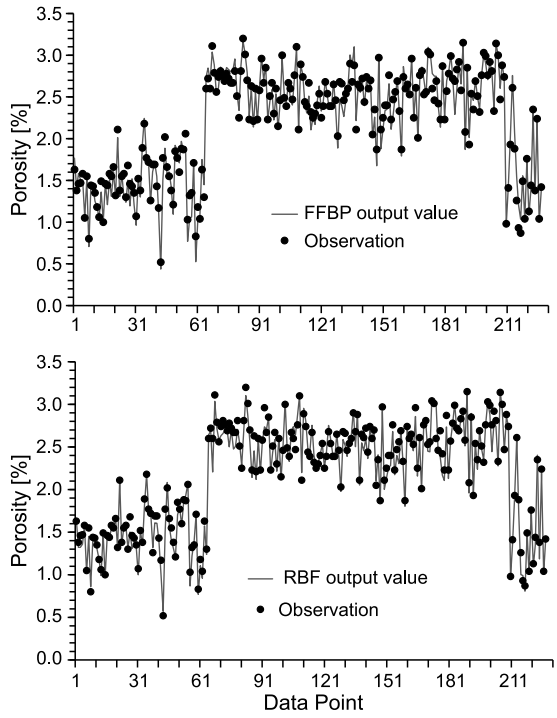

Fig. 4. Fit of the feed-forward backpropagation (FFBP) neural network and radial basis function (RBF) neural network learning schemes with observations based on the training data.

Table 4. Statistical performance of the feed-forward backpropagation neural network and radial basis function neural network models using the training data. *MSE* - mean squared error, R^2 - coefficient of determination.

Model	*MSE*	R^2
FFBP	0.011	0.968
RBF	0.009	0.979

Though not included here, training and testing using FFBP and RBF were carried out to explore all possible combinations of inputs. The results showed that the prediction became more inaccurate when *CNL* was added to the actual panel of input parameters; possibly because *CNL* is not a good indicator of porosity prediction. As can be seen in Table 3, the probability of correlation coefficient between measured porosity and *CNL* (0.554) is higher than the level of significance (0.01). The hypothesis of linearity is not supported and the nonexistence of relationship is not caused by nonlinearity. This is not a surprising effect, it has been mentioned by *Bartetzko et al. (2005)* that *CNL* cannot be used as a porosity indicator in crystalline rocks, providing porosity values that are greatly

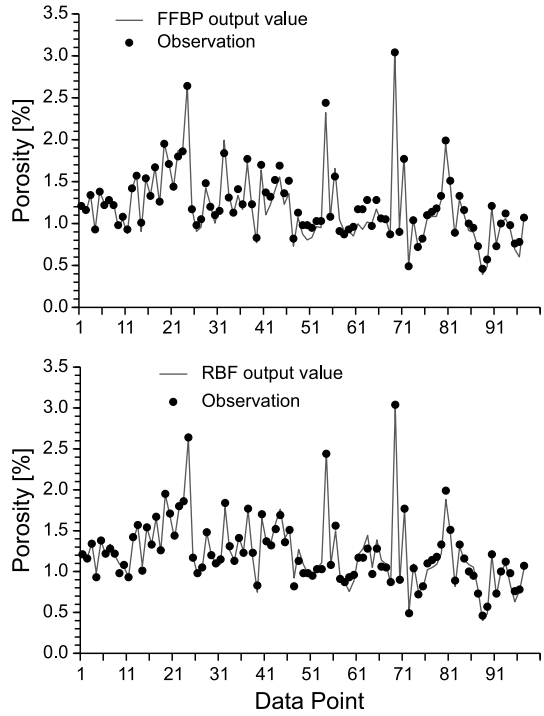

Fig. 5. The same as in Fig. 4, but for the test data.

Table 5. The same as in Table 4, but for the test data.

Model	*MSE*	R^2
FFBP	0.006	0.968
RBF	0.003	0.978

higher than the porosity of the rocks. In this case, it was impossible to build up a performance model that includes *CNL*.

Based on any modeling approach, it is a good idea to assess the model's power. Statistical diagnostics allow us to detect patterns that are poorly predicted by ANNs. Keeping this in mind, careful examination of the distribution of relative residuals of porosity was done to demonstrate that if results from the actual ANN schemes were acquired purely by chance i.e. noise, or if the ANN schemes were learning from the three geophysical logs.

Relative residuals are defined as:

$$R_r^i = \frac{\Phi_{oi} - \Phi_{pi}}{\Phi_{oi}}, \tag{13}$$

where Φ_{oi} is the measured and Φ_{pi} the predicted porosity, respectively.

The distribution of relative residuals of a good model is normally distributed. Fig. 6 depicts an approximately normal distribution of relative residuals made by the FFBP and RBF models for porosity estimation. We have applied a normal density function on the histograms. Based on this analysis, we have demonstrated that the sonic, density and resistivity, combined into an ANN provide accurate porosity estimates in CCSD-MH. It can be obviously concluded in this study, that the ANNs have predicted porosity from the logging tools responses i.e. from the three geophysical logs.

After successfully testing on data not covered by the training (testing data), the two ANN models were evaluated on all data. Fig. 7 illustrates the comparison between the networks and target value from all data. Referring to Fig. 7 it appears that in general there is a satisfactory fit between the porosity predicted by ANN models and the corresponding observed porosity. These results can be explained by the fact that by matching geophysical well logs with core porosity, ANNs have judiciously established a robust physical relationship between the input (geophysical well logs) and output (porosity). Therefore, it can be said that, ANNs are not strongly affected by rock composition change; since they have predicted porosity satisfactorily, despite the complex features and nonlinearity in the crystalline crust, such as CCSD-MH.

Considering the results in Table 6, it appears that RBF fits much better the porosity than the FFBP. Both RBF and FFBP are three-layered networks; the difference between them exists in the handling of nonlinearities in the hidden units. Tangent hyperbolic function was used in FFBP while function Gaussian function was used in RBF. It is shown in Table 6, that the model for better capturing non-linearities was the RBF, since it has archived the best results of each performance indicator (*MSE* and R^2). Thus, RBF was able to predict porosity along CCSD-MH more successfully.

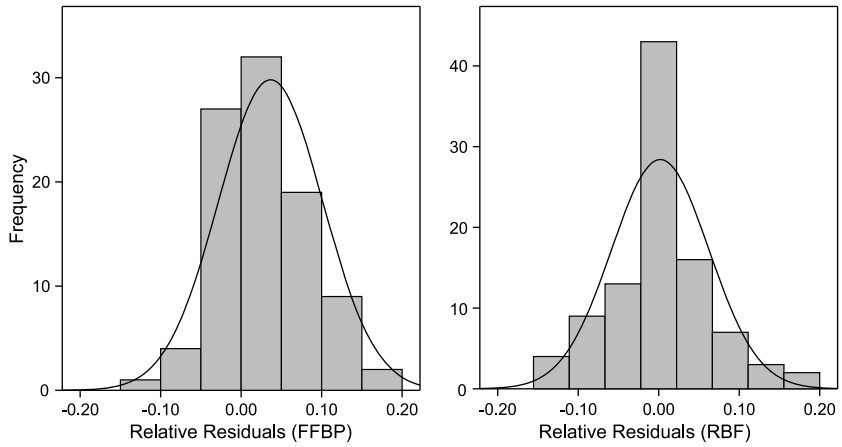

Fig. 6. Distribution of relative residuals (Eq. (13)) obtained by the feed-forward backpropagation (FFBP) neural network and radial basis function (RBF) neural network learning schemes for porosity estimation using the test data.

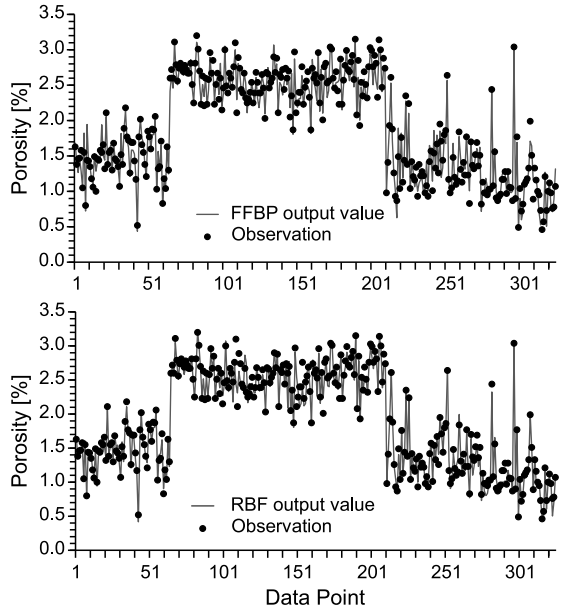

Fig. 7. Comparison between network output and observations for the feed-forward backpropagation (FFBP) neural network and radial basis function (RBF) neural network using all data.

Table 6. The statistical performance of artificial neural networks and regression models using all data. *MSE* - mean squared error, *R* - Pearson correlation coefficient, FFBP - feed-forward backpropagation neural network, RBF - radial basis function neural network, PIR - piecewise regression, POR - polynomial regression, IMLR - interaction multi-linear regression, MLR - multi-linear regression.

Model	*MSE*	R^2	*R*
FFBP	0.015	0.969	0.984
RBF	0.010	0.979	0.989
PIR	0.086	0.831	0.911
POR	0.359	0.293	0.541
IMLR	0.366	0.281	0.530
MLR	0.378	0.256	0.506

In order to compare the current technique (ANN) to the regression technique, we also performed several regression models (linear and nonlinear transformation) to predict porosity from *RSFL*, *DEN* and *AC* logs. Only we selected models which gave better performance in terms of R^2 and *MSE* among several models. Therefore, we retained four models based: a multi-linear regression (MLR), a interaction multi-linear regression (IMLR), a polynomial regression (POR) and a piecewise regression (PIR) represented by Eqs (14)–(17), respectively:

$$y = -3.137 + 0.053\,AC + 0.691\,DEN + 19\times10^{-5}\,RSFL\,, \tag{14}$$

$$y = -12.331 + 0.239\,AC + 4.025\,DEN - 8\times10^{-4}\,RSFL \\ -0.068\left(AC \times DEN\right) + 1\times10^{-4}\left(DEN \times RSFL\right), \tag{15}$$

$$y = -0.387 + 0.137\,AC - 3.172\,DEN + 3\times10^{-5}\,RSFL \\ -67\times10^{-5}\left(AC \times AC\right) + 0.697\left(DEN \times DEN\right), \tag{16}$$

$$y = \begin{cases} 0.683 + 0.007\,AC + 0.047\,DEN + 89\times10^{-6}\,RSFL & \text{for } y \le \text{breakpoint}, \\ 2.010 + 0.004\,AC + 0.110\,DEN + 9\times10^{-6}\,RSFL & \text{for } y > \text{breakpoint}, \end{cases} \tag{17}$$

where y is the predicted (expected) value, *AC*, *DEN* and *RSFL* are distinct independent variables (well logs), and the break point is 1.90. Comprehensible theory of the regression techniques can be found *Anderson (1984)*; *Liu et al. (1997)*; *Seber and Wild (1989)*; *Aiken and West (1991)*; *Muggeo (2003)*; *Montgomery et al. (2006)*.

As shown in Table 6, a piecewise regression (PIR) model archived the highest performance among the regression models. Since it exhibits the highest R^2 and lowest *MSE* values. Based on these results, we can say that the MLR, IMLR and PR models do not handle the predicting of porosity in optimal way. On the other hand, in comparing regression techniques to ANNs, Table 6 depicts that the ANNs models show better performance than the regression models whether *AC*, *DEN* and *RSFL* logs are used as inputs. The proposed ANNs show higher R^2 and lower *MSE* value. Whereas lower R^2 and higher *MSE* value are achieved applying regression techniques. Additionally, Fig. 8 clearly shows the closeness of fit of ANN models to the observed porosity as compared to the best regression model (PIR model). From these results, we conclude that ANN models were more appropriate for capturing the non-linearity of the relationship between porosity and well logs in the context of CCSD-MH data.

In comparison to earlier published papers, the correlation coefficient of porosity by *Pechnig et al. (1997)* using linear regression was 0.75 and by *Zimmermann et al. (1992)* using multiple regression were 0.80 and 0.88. While in this study, as shown in Table 6, the results obtained from ANNs models are greater; and the correlation of porosity by FFBP and RBF were 0.984 and 0.989 respectively. These higher values indicates that ANN approach is more powerful and accurate than regression approaches. However, it is important to note that ANN is black box model which do not allow interpretation between input and output relationship (*Dreiseitl and Ohno-Machado, 2002*). In the present context, interpretation of functional relationship between porosity and geophysical logs is impossible. In contrast the regression analysis helps in the interpretation of this relationship. But, computer programs that use a statistical method cannot learn or become smarter (*Lopez et al., 2005*) to discover input-output relationship as compared to the intelligence technique used in this study.

Prediction porosity in the framework of research drillings in continental crust, crystalline rock is not an easy task, but in this paper an innovative challenge was made in the modelling based on two ANNs which includes FFBP and RBF. The objective of prediction was simply to demonstrate that matching geophysical well logs and core data could develop a model and enhance accuracy in predicting the porosity of the crystalline crust.

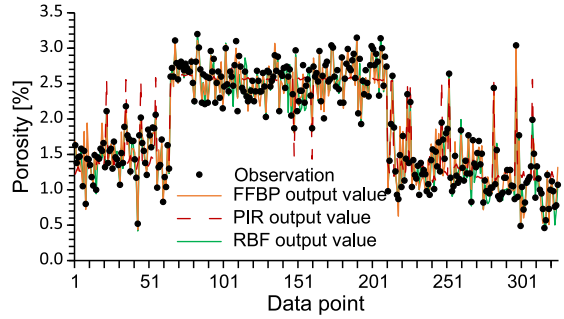

Fig. 8. Comparison of neural networks and piecewise regression methods in the porosity prediction. FFBP - feed-forward backpropagation neural network, PIR - piecewise regression, RBF - radial basis function neural network.

7. CONCLUSIONS

This study sought to explore and address concerns encountered by geophysicists in the framework of research drillings in continental crust by considering the application of artificial neural networks (ANN) in analyzing the Chinese Continental Scientific Drilling Main Hole (CCSD-MH) logging data. To this end, feed-forward backpropagation neural network (FFBP) and radial basis function network (RBF) models have been presented to predict the porosity of rock by four geophysical well logs (density, neutron porosity, sonic and resistivity).

On the CCSD-MH data, the findings showed that, procedural differences in predicting of FFBP and FBNN are all talented to offer satisfactory prediction of porosity using sets of three geophysical well logs (density, sonic and resistivity). ANNs are therefore a talented technique for quick and efficient porosity predictions in framework of research drillings.

In comparison to FFBP, the RBF exhibits superior stability and more accurate results; since it results in lower mean squared error (*MSE*) and higher coefficient of determination (R^2). It can be suggested that RBF be used instead of FFBP in porosity modeling in the framework of research drillings in continental crust.

Comparison of ANNs to regression technique showed that ANNs provide better performance with sets of three geophysical well logs (density, sonic and resistivity) than regression technique.

The idea behind this study is not to remove the expertise and interpretive experience of a qualified geophysicist but to show how the task can be simplified and made more effective. In this way geophysicists are able to focus on the important information.

This study will provide a better understanding of the modeling technique of ANN and their relevance in the analysis of CCSD-MH. Last, but not least, it will add a new dimension to the existing knowledge and will be useful to the geoscientist community.

From our point of view, it is fair to say that no work ever covers all of the research that the researchers envisaged covering when they started the project. The same is true for this work. In utilizing neural networks, the whole available data set is generally randomly

divided into training and testing sets. Training set is used to construct the model and testing set is used to evaluate how the model behave on unseen data. While this practice is implemented in many studies, any bias resulting to the inappropriate split of whole dataset may generate a negative impact on the performance of ANN (*Van der Baan and Jutten, 2000*). In other perspective, the predicted value can be very different from the target value mainly when small sample sizes are concerned. Besides, most importantly, for training-testing scheme, the hold-out sampling is commonly performed only once during ANN development (*May et al., 2010*). In this sense, the model generalization ability may not be guaranteed. For this reason, future directives in improving ANN generalization ability is a major significance. Based on this, we see the resampling techniques such as *k*-fold cross-validation, jackknife and bootstrap in which future work can done. They are essential tools to enhance a predictor performance. Resampling techniques are computer intensive techniques which imply repeatedly drawing samples from a dataset and refitting a model of interest on each sample to achieve additional information about the fitted model. This technique will give valuable understandings on the reliability of the ANNs with regard to sampling rotation. Book-length dealings on resampling methods can be found in *Shao and Tu (1995)* and *Good (2006)*. Next, RBF model could be additional exploited for investigating of porosity in some other geologically complex zone of interest. Moreover, we are expected to see the application of new types of computational tool to CCSMH data.

Acknowledgements: This work was funded by the Chinese Continental Scientific Drilling (CCSD) of National "Ninth Five" major scientific projects. We appreciated helpful comments from Prof. G. Randy Keller and anonymous reviewers.Special thanks goes to Mr. Rohan Wright and Ms. Margaret Oloo for improving the English in our manuscript.

References

Aiken L.S. and West S.G., 1991. *Multiple Regression: Testing and Interpreting Interactions*. Sage Publ. Inc., Thousand Oaks, CA.

Anderson T.W., 1984. *An Introduction to Multivariate Statistical Analysis*. 2nd Edition. John Wiley&Sons, New York.

Anderson R.N., Alt J.C., Malpas J., Lovell M.A., Harvey P.K. and Pratson E.L., 1990. Geochemical well logging in basalts: The palisade sill and the oceanic crust of hole 504B. *J. Geophys Res*., **90**, 9265–9292.

Baddari K., Aıfa T., Djarfour N. and Ferahtia J., 2009. Application of a radial basis function artificial neural network to seismic data inversion. *Comput. Geosci.*, **35**, 2338–2344.

Baldwin J.L., Bateman A.R.M. and Wheatley C.L., 1990. Application of neural networks to the problem of mineral identification from well-logs. *The Log Analyst*, **3**, 279–293.

Bartetzko A., Delius H. and Pechnig R., 2005. Effect of compositional and structural variations on log responses of igneous and metamorphic rocks. I: mafic rocks. In: Harvey P.K., Brewer T.S., Pezard P.A. and Petrov V.A (Eds), *Petrophysical Properties of Crystalline Rocks*. *Geol. Soc. London Spec. Publ.*, **240**, 255–278.

Benaouda D., Wadge G., Whitmarsh R.B., Rothwell R.G. and MacLeod C., 1999. Inferring the lithology of borehole rocks by applying neural network classifiers to downhole logs: an example from the Ocean Drilling Program. *Geophys. J. Int.*, **136**, 477–491.

Benoudjit N. and Verleysen M., 2003, On the kernel widths in radial-basis function networks. *Neural Process. Lett.*, **18**, 139–154.

Bhatt A., 2002. *Reservoir Properties from Well Logs Using Neural Networks*. Ph.D. Thesis, Norwegian University of Science and Technology, Trondheim, Norway.

Bhatt A. and Helle H.B., 2002. Committee neural networks for porosity and permeability prediction from well logs. *Geophys. Prospect.*, **50**, 645–660.

Bishop C., 1995. *Neural Networks for Pattern Recognition*. Oxford University Press, Oxford, U.K.

Celikoglu H.B., 2006. Application of radial basis function and generalized regression neural networks in non-linear function specification for travel mode choice modelling. *Math. Comput. Model.*, **44**, 640–658.

Chang H.C., Merkel Kopaska D.C., Chen H.C. and Durrans S.R., 2000. Lithofacies identification using multiple adaptive resonance theory neural networks and group decision expert system. *Comput. Geosci.*, **26**, 591–601.

Dreiseitl S. and Ohno-Machado L., 2002. Logistic regression and artificial neural network classification models: a methodology review. *J. Biomed. Inform.*, **35**, 352–359.

Good P.I., 2006. *Resampling Methods*. 3rd Edition. Birkhauser, Boston, PA.

Hagan M.T. and Menhaj M.B., 1994. Training feedforward techniques with the Marquardt algorithm. *IEEE Trans. Neural Netw.*, **5**, 989–993.

Harvey P.K., Brewer T.S., Pezard P.A. and Petrov V.A. (Eds), 2005. *Petrophysical Properties of Crystalline Rocks*. *Geol. Soc. London Spec. Publ.*, **240**.

Haykin S., 1998. *Neural Networks: A Comprehensive Foundation*. Prentice-Hall, New Jersey.

Helle H.B., Bhatt A. and Ursin B., 2001. Porosity and permeability prediction from wireline logs using artificial neural networks: a North Sea case study. *Geophys. Prospect.*, **49**, 431–444.

Hornik K., Stinchcombe M.B. and White H., 1989. Multilayer feed-forward networks are universal approximators. *Neural Netw.*, **2**, 359–366.

Ji S.C. and Xu Z.Q., 2009. Drilling deep into the ultrahigh pressure (UHP) metamorphic terrane. *Tectonophysics*, **475**, 201–203.

Ji S.C., Wang Q., Marcotte D., Salisbury M.H. and Xu Z.Q., 2007. P-wave velocities, anisotropy and hysteresis in ultrahigh-pressure metamorphic rocks as a function of confining pressure. *J. Geophys. Res.*, **112**, B09204, DOI: 10.1029/2006JB004867.

Kern H., Jin Z.M., Shan Gao S., Popp T. and Xu Z., 2002. Physical properties of ultrahigh-pressure metamorphic rocks from the Sulu terrain, eastern central China: implications for the seismic structure at the Donghai (CCSD) drilling site.*Tectonophysics*, **354**, 315–330.

Levenberg K., 1944. A method for the solution of certain non-linear problems in least squares. *Q. Appl. Math.*, **2**, 164–168.

Liu J., Wu S. and Zidek J.V., 1997. On segmented multivariate regression. *Stat. Sin.*, **7**, 497–525.

Liu F.L., Xue H.M., Xu Z.Q., Liang F.H. and Gerdes A., 2006. SHRIMP U-Pb zircon dating from eclogite lens in marble, Shuanghe area of Dabie UHP terrane: restriction on prograde, UHP and retrograde metamorphic ages. *Acta Petrol. Sinica*, **22**, 1761–1778.

Liu Q., Zeng Q., Zheng J., Yang T., Qiu N., Liu Z., Luo Y. and Jin Z., 2010. Magnetic properties of serpentinized garnet peridotites from the CCSD main hole in the Sulu ultrahigh-pressure metamorphic belt, eastern China. *J. Geophys. Res*, **115**, B06104, DOI: 10.1029 /2009JB000814.

Lopez G., Batlles F.J. and Tovar-Pescador J., 2005. Selection of input parameters to model direct solar irradiance by using artificial neural networks. *Energy*, **30**, 1675–1684.

Luo M. and Pan H.P, 2010. Well logging responses of UHP metamorphic rocks from CCSD Main Hole in Sulu Terrane, Eastern Central China. *J. Earth Sci.*, **21**, 347–357, DOI: 10.1007/s12583-010-0098-9.

Luo M. and Pan H.P., 2011. Resistivity logs of the Chinese Continental Scientific Drilling Main Hole: implication for the crustal electrical structure of Dabie-Sulu Terrane, Central-Eastern China. *J. Earth Sci.*, **22**, 292–298, DOI: 10.1007/s12583-011-0182-9.

Luthi S.M. and Bryant I.D., 1997. Well-log correlation using a back-propagation neural network. *Math. Geol.*, **29**, 413–425.

Maiti S., Tiwari R.K. and Kumpel H.J., 2007. Neural network modelling and classification of lithofacies using well log data: a case study from KTB borehole site. *Geophys. J. Int.*, **169**, 733–746.

Maiti S. and Tiwari R.K., 2009. A hybrid Monte Carlo method based artificial neural networks approach for rock boundaries identification: a case study from KTB Borehole. *Pure Appl. Geophys.*, **166**, 2059–2090, DOI: 10.1007/s00024-009-0533-y.

Maiti S. and Tiwari R.K., 2010. Neural network modeling and an uncertainty analysis in Bayesian framework:A case study from the KTB borehole site. *J. Geophys. Res.*, **115**, B10208, DOI: 10.1029/2010JB000864.

May R.J., Maier H.R. and Dandy G.C., 2010. Data splitting for artificial neural networks using SOM- based stratified sampling. *Neural Netw.*, **23**, 283–294.

Meng X.H., Yu Q.F., Guo Y.Z. and Zhou Y.X., 2007. A preliminary study on paleomagnetism and rock magnetism of Eclogite from the Maobei area. *J. China Univ. Geosci.*, **18**, 366–374.

Montgomery D.C., Peck E.A., Vining G.G., 2006. Introduction to Linear Regression Analysis, 4th edition, Wiley-Interscience Publication.

Moody J. and Darken C.K., 1989. Fast learning in networks of locally-turned processing units. *Neural Comput.*, **1**, 281–294.

Moos D., 1990. Utilization of observations of well bore failure to constrain the orientation and magnitude of crustal stresses: Application to continental, Deep Sea Drilling Project, and Ocean Drilling Program boreholes. *J. Geophys Res.*, **95(B6)**, 9305–9325.

Moritz E., Bornholdt S., Westphal H. and Meschede M., 2000. Neural network interpretation of LWD data (ODP Leg 170) confirms complete sediment subduction at the Costa Rica convergent margin. *Earth Planet. Sci. Lett.*, **174**, 301–331.

Muggeo V.M.R., 2003. Estimating regression models with unknown break-points. *Statist. Med.*, **22**, 3055–3071, DOI: 10.1002/sim.1545.

Niu X.Y., Pan H.P., Wang W.X., Zhu L.F. and Xu D.H., 2004. Geophysical well logging in main hole (0–2000 m) of Chinese Continental Scientific Drilling. *Acta Petrol. Sin.*, **20**, 109–118 (in Chinese with English abstract).

Ou X.G., Jin Z.M., Xia B., Xu H.J. and Jin S.Y., 2005. Correlations between petrophysical properties of the UHP rocks and its significance on establishing the geophysical interpretation standards for crystalline rocks. *Acta Petrol. Sin.*, **21**, 1005–1014.

Pan H.P., Luo M. and Zhao Y., 2010. Identification of metamorphic rocks in the CCSD Main Hole. In: Yue S., Wei H.L., Wang L. and Song Y. (Eds), *2010 Sixth International Conference on Natural Computation*. IEEE, 4049–4051.

Pan H.P., Niu, Y.X. and Wang W.X., 2002. CCSD well logging engineering program. *J. China Univ. Geosci.*, **13**, 91–94.

Pan H.P., Niu Y.X. and Wang W.X., 2005. Radioactive logging application in CCSD Main Hole. *Earth Sci.-J. China Univ. Geosci.*, **30(Suppl.)**, 49–56 (in Chinese with English Abstract).

Park J. and Sandberg I., 1993. Approximation and radial basis function networks. *Neural Comput.*, **5**, 305–316.

Pechnig R., Delius H. and Bartetzko A., 2005. Effect of compositional variations on log responses of igneous and metamorphic rocks. II: acid and intermediate rocks. In: Harvey P.K., Brewer T.S., Pezard P.A. and Petrov V.A. (Eds), *Petrophysical Properties of Crystalline Rocks*. *Geol. Soc. London Spec. Publ.*, **240**, 279–300.

Pechnig R., Heaverkamp S. and Wohlenberg J., 1997. Integrated log interpretation in the German Continental Deep Drilling Program: lithology, porosity, and fracture zones. *J. Geophys Res*., **102(B8)**, 8363–18390.

Poulton M.M., 2002. Neural networks as an intelligence amplification tool: A review of applications. *Geophysics*, **67**, 979–993.

Pratsone E.L., Anderson R.N., Dove R.E., Lyle M., Silver L.T., James E.J. and Chappell B.W., 1992. Geochemical logging in the Cajon Pass drillhole and a new, oxide, igneous rock classification scheme. *J. Geophys Res*., **97**, 5167–5180.

Reynaldi A., Lukas S. and Margaretha H., 2012. Backpropagation and Levenberg-Marquardt algorithm for training finite element neural network. In: El-Dabass E., Debono C., Muscat R., Adithia N., Basuki T. and Orsoni A. (Eds), *Proceedings, UKSim-AMSS, 6th European Modelling Symposium*. IEEE, 89–94, DOI: 10.1109/EMS.2012.56.

Seber G.A.F. and Wild C.J., 1989. *Nonlinear Regression*. John Wiley&Sons, New York.

Serra O., 2007. *Well Logging and Reservoir Evaluation*. Editions Technip, Paris, France.

Shao J. and Tu D., 1995. *The Jackknife and Bootstrap*. Springer-Verlag, New York.

Sun S.S., Ji S.C., Wang Q., Salisbury M. and Kern H., 2012. P-wave velocity differences between surface-derived and core samples from the Sulu ultrahigh-pressure terrane: Implications for in situ velocities at great depths. *Geology*, **40**, 651–654, DOI: 10.1130/G33045.

Tullborg E.L. and Larson S.A, 2006. Porosity in crystalline rocks - a matter of scale. *Eng. Geol.*, **84**, 75–83.

Van der Baan M. and Jutten C., 2000. Neural networks in geophysical applications. *Geophysics*, **65**, 1034–1047.

Wang Q., Ji S.C., Salisbury M.H., Xia B., Pan M.B. and Xu Z.Q., 2004. Pressure dependence and anisotropy of P-wave velocities in ultrahigh-pressure metamorphic rocks from the Dabie-Sulu orogenic belt (China): Implications for seismic properties of subducted slabs and origin of mantle reflections. *Tectonophysics*, **398**, 67–99.

White H., 1992 *Artificial Neural Networks. Approximation and Learning Theory*. Blackwell, Cambridge, MA.

Xu P.F., Liu F.T., Wang Q.C., Cong B.L., Chen H. and Sun R.M., 2000. Seismic tomography beneath the Dabie-Sulu collision orogeny - 3D velocity structures of lithosphere. *Chin. J. Geophys.*, **43**, 377–385 (in Chinese with English Abstract).

Xu S., Okay A.I., Ji S., Sengor A.M.C., Su W., Liu Y. and Jiang L., 1992. Diamond from the Dabie Shan metamorphic rocks and its implication for tectonic setting. *Science*, **256**, 80–82.

Xu Z.Q., Yang W.C., Ji S.C., Zhang Z.M., Yang J.S., Wang Q. and Tang Z.M., 2009. Deep root of a continent-continent collision belt: Evidence from the Chinese Continental Scientific Drilling (CCSD) deep borehole in the Sulu ultrahigh-pressure (HP-UHP) metamorphic terrane, China. *Tectonophysics*, **475**, 204–219.

Yang W.C., 2009. The crust and upper mantle of the Sulu UHPM belt. *Tectonophysics*, **475**, 226–234.

Zimmermann G., Burkhardt H. and Meichert M., 1992. Estimation of porosity in crystalline rock by a multivariate statistical approach. *Sci. Drill.*, **3**, 27–37.

Zoveidavianpoor M., Samsuri A. and Shadizadeh S.R., 2013. Prediction of compressional wave velocity by an artificial neural network using some conventional well logs in a carbonate reservoir. *J. Geophys. Eng*., **10**, 045014, 1–13, DOI: 10.1088/1742-2132/10/4/045014.